A framework for quantifying the impacts of sub-pixel reflectance variance and covariance on cloud optical thickness and effective radius retrievals based on the bi-spectral method

Z. Zhang, F. Werner, H.-M. Cho, G. Wind, S. Platnick, A. S. Ackerman, L. Di Girolamo, A. Marshak, and Kerry Meyer

Citation: AIP Conference Proceedings **1810**, 030002 (2017); doi: 10.1063/1.4975502
View online: https://doi.org/10.1063/1.4975502
View Table of Contents: http://aip.scitation.org/toc/apc/1810/1
Published by the American Institute of Physics

A Framework For Quantifying The Impacts Of Sub-Pixel Reflectance Variance And Covariance On Cloud Optical Thickness And Effective Radius Retrievals Based On The Bi-Spectral Method

Z. Zhang[1,2,a)], F. Werner[2], H.-M. Cho[2,3], G. Wind[4,5], S. Platnick[4], A. S. Ackerman[6], L. Di Girolamo[7], and A. Marshak[4], Kerry Meyer[4,8]

[1]*Physics Department, UMBC, Baltimore, MD, USA*
[2]*Joint Center for Earth Systems Technology, UMBC, Baltimore, MD, USA*
[3]*Electronics and Telecommunications Research Institute, Korea*
[4]*NASA Goddard Space Flight Center, Greenbelt, MD, USA*
[5]*Science Systems and Applications, Inc., Maryland 20706, USA*
[6]*NASA Goddard Institute for Space Studies, New York City, NY, USA*
[7]*Department of Atmospheric Sciences, University of Illinois, Urbana-Champaign, IL, USA*
[8]*Universities Space Research Association (USRA), Columbia, MD, USA*

[a)]*Corresponding author: zzbatmos@umbc.edu*

Abstract. The so-called bi-spectral method retrieves cloud optical thickness (τ) and cloud droplet effective radius (r_e) simultaneously from a pair of cloud reflectance observations, one in a visible or near infrared (VIS/NIR) band and the other in a shortwave-infrared (SWIR) band. A cloudy pixel is usually assumed to be horizontally homogeneous in the retrieval. Ignoring sub-pixel variations of cloud reflectances can lead to a significant bias in the retrieved τ and r_e. In this study, we use the Taylor expansion of a two-variable function to understand and quantify the impacts of sub-pixel variances of VIS/NIR and SWIR cloud reflectances and their covariance on the τ and r_e retrievals. This framework takes into account the fact that the retrievals are determined by both VIS/NIR and SWIR band observations in a mutually dependent way. In comparison with previous studies, it provides a more comprehensive understanding of how sub-pixel cloud reflectance variations impact the τ and r_e retrievals based on the bi-spectral method. In particular, our framework provides a mathematical explanation of how the sub-pixel variation in VIS/NIR band influences the r_e retrieval and why it can sometimes outweigh the influence of variations in the SWIR band and dominate the error in r_e retrievals, leading to a potential contribution of positive bias to the r_e retrieval.

INTRODUCTION

Among many satellite-based cloud remote sensing techniques, the bi-spectral solar reflective method ("bi-spectral method" hereafter) is a widely used method to infer cloud optical thickness (τ) and cloud droplet effective radius (r_e) from satellite observation of cloud reflectance[1]. The bi-spectral method makes several important assumptions about the cloud (or cloudy pixels). Most important of all, cloud is assumed to be horizontally homogenous (referred to as the "homogenous pixel assumption") within a cloudy pixel. The focus of this study is to develop a unified framework for understanding and quantifying the impacts of sub-pixel level unresolved reflectance variations on r_e and τ retrievals based on the bi-spectral method. A number of previous studies have already made substantial progresses in this direction. It has been known for a long time that at the spatial scale of climate model grids (e.g., ~ 10^2 km) approximating inhomogeneous cloud fields with plane-parallel clouds can lead

AIP Conf. Proc. 1810, 030002-1–030002-6; doi: 10.1063/1.4975502
Published by AIP Publishing. 978-0-7354-1478-5/$30.00

to significant biases in shortwave solar radiation [e.g., 2-4]. *Cahalan et al.* [3] described an elegant theoretical framework based on a fractal cloud model to explain the influence of small-scale horizontal variability of τ on the averaged cloud reflectance in the visible spectral region R_{VIS}. It is shown that the averaged reflectance $\overline{R_{VIS}(\tau_i)}$, where τ_i denotes the sub-pixel scale cloud optical thickness, is smaller than the reflectance that corresponds to the averaged cloud optical thickness $\overline{\tau_i}$, i.e., $\overline{R_{VIS}(\tau_i)} < R_{VIS}(\overline{\tau_i})$. This inequality relation is well known as the "plane-parallel homogenous bias" (referred to as PPHB), which is a result of the non-linear dependence of R_{VIS} on τ i.e., $\frac{\partial^2 R_{vis}}{\partial \tau^2} < 0$. The implication of the PPHB for τ retrievals from R_{VIS} is illustrated using an example shown in **Fig. 1**a. Here, we assume that one half of an inhomogeneous pixel is covered by a thinner cloud with $\tau_1 = 5$ and the other half by a thicker cloud with $\tau_2 = 18$ (both clouds with $r_e = 8\mu m$). Because of the PPHB, the retrieved cloud optical thickness $\tau^* = 9.8$ based on the averaged reflectance $\overline{R} = \left[R(\tau_1) + R(\tau_2)\right]/2$ is significantly smaller than the linear average of the sub-pixel τ, i.e., $\overline{\tau} = 11.5$. The impacts of PPHB on satellite based cloud property retrievals and the implications have been investigated in a number of studies [5-7]. Marshak et al. [8] pointed out that similar to the PPHB the non-linear dependence of the SWIR band cloud reflectance R_{SWIR} on r_e can also lead to significant biases on r_e retrievals, which is demonstrated in **Fig. 1**b. Here, one half of an inhomogeneous pixel is covered by a cloud with $r_e = 8\mu m$ and the other half by a cloud with $r_e = 22\mu m$. Both parts have the same $\tau = 4.1$. As shown in the figure, the retrieved $r_e^* = 12\mu m$ based on the averaged reflectance is significantly smaller than the linear average of sub-pixel $\overline{r_e} = 15\mu m$, similar to the PPHB of τ in **Fig. 1** a.

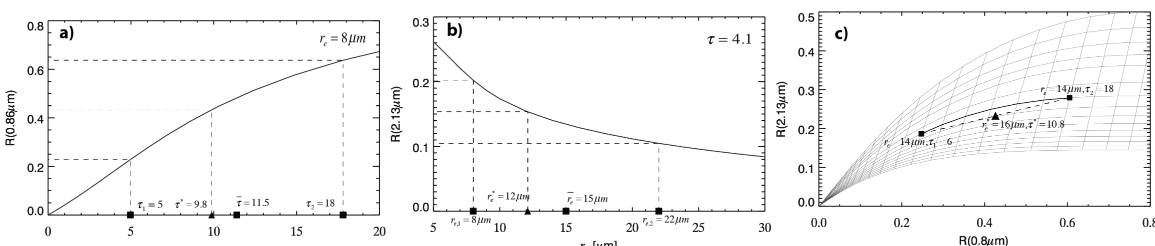

FIGURE 1 a) an example to illustrate the PPHB bias proposed in Cahalan et al. [3] for τ retrieval, b) example to illustrate the PPHB bias proposed in Marshak et al. [8], c) example to illustrate the r_e retrieval bias caused by sub-pixel τ variability proposed in Zhang and Platnick [9] and Zhang et al. [10]. See text for details. Solar and view zenith angles are assume to be 20° and 0° and relative azimuth angle is assumed to be 30° in these cases. (This figure is from Zhang et al. 2016 [11])

It must be noted that in the framework of Marshak et al. [8] the retrievals of r_e and τ are considered separately and assumed to be independent from one another. However, as Marshak et al. [8] pointed out this assumption is valid only for "large enough" τ and r_e (typically, $r_e > 5$ μm and $\tau > 10$). However, the R_{SWIR} is not completely orthogonal to the R_{VIS}, especially when τ is small. As a result, the retrievals of r_e and τ are not independent from one another. Marshak et al. [8] suspected that some cases with large r_e bias in their simulations might be the result of this mutual dependence of r_e and τ retrievals. Recently, Zhang and Platnick [9] showed that the sub-pixel variance of τ can have a significant impact on the r_e retrieval, which is illustrated in the example in **Fig. 1**c. In this hypothetical case, an inhomogeneous pixel is assumed to be covered by a thinner cloud with τ_1=6 in one half and a thicker cloud with τ_2=18 in the other. Both clouds have the same r_e=14 μm. Note that in this case the sub-pixel reflectance variation is solely caused by the variability in t. If the r_e retrieval were independent from the τ retrieval, then the retrieved r_e would be 14 μm. The solid triangle in the figure indicates the location of the R_{VIS} and R_{SWIR}

averaged over the pixel, i.e., the "observation". The retrieved $\tau^* = 10.8$ is smaller than the averaged $\overline{\tau} = 12$ as a result of the PPHB. However, the retrieved $r_e^* = 16$ is 2 µm larger than the expected value of 14 µm. This positive bias in the r_e retrieval, apparently caused by the sub-pixel variability of τ, cannot be explained by the framework of Marshak et al. [8] in which the r_e retrieval is assumed to be independent from the τ retrieval. Zhang and Platnick [9] and Zhang et al. [10] also found that the magnitude of the positive r_e retrieval bias caused by the sub-pixel variability of τ is dependent on the SWIR band chosen for the r_e retrieval.

STATEMENT OF THE PROBLEM

In the bi-spectral method, r_e and τ are retrieved from a pair of cloud reflectance observations, one in VIS/NIR and the other in SWIR. From this point of view, we can define r_e and τ as:

$$\begin{aligned} \tau &\equiv \tau\left(R_{VIS}, R_{SWIR}\right) \\ r_e &\equiv r_e\left(R_{VIS}, R_{SWIR}\right) \end{aligned}, \tag{1}$$

where R_{VIS} and R_{SWIR} are the observed reflectances in the VIS/NIR (denoted by subscript "VIS" for short) and SWIR bands, respectively. Assume that an instrument with a relatively coarse spatial resolution observes a horizontally inhomogeneous cloudy pixel in its field of view. The observed cloud reflectances are $\overline{R_{VIS}}$ and $\overline{R_{SWIR}}$, where the overbar denotes the spatial average. Now if we use another instrument with a finer spatial resolution to observe the same area covered by the coarser resolution pixel, we can obtain high-resolution observations, $R_{VIS,i}$ and $R_{SWIR,i}, i = 1,2,\ldots N$, (the number N depends on the relative sizes of the pixels). The high-resolution measurements provide the information on the variance and covariance of R_{VIS} and R_{SWIR} at sub-pixel scale. Each sub-pixel observation $R_{VIS,i}$ and $R_{SWIR,i}$ can be specified as the deviation from the mean value $\overline{R_{VIS}}$ and $\overline{R_{SWIR}}$ as:

$$\begin{aligned} R_{VIS,i} &= \overline{R_{VIS}} + \Delta R_{VIS,i} \\ R_{SWIR,i} &= \overline{R_{SWIR}} + \Delta R_{SWIR,i} \end{aligned} \quad ; i = 1,2 \ldots N . \tag{2}$$

It naturally follows that the spatial average $\overline{\Delta R_{VIS,i}} = \overline{\Delta R_{SWIR,i}} = 0$. Based on the coarse-resolution reflectance observations $\overline{R_{VIS}}$ and $\overline{R_{SWIR}}$, we can retrieve $\tau\left(\overline{R_{VIS}}, \overline{R_{SWIR}}\right)$ and $r_e\left(\overline{R_{VIS}}, \overline{R_{SWIR}}\right)$. From the high-resolution, sub-pixel observations $R_{VIS,i}$ and $R_{SWIR,i}$, we can retrieve $\tau\left(R_{VIS,i}, R_{SWIR,i}\right)$ and $r_e\left(R_{VIS,i}, R_{SWIR,i}\right)$. The differences $\Delta\tau$ and Δr_e, defined as:

$$\begin{aligned} \Delta\tau &= \tau\left(\overline{R_{VIS}}, \overline{R_{SWIR}}\right) - \overline{\tau\left(R_{VIS,i}, R_{SWIR,i}\right)} \\ \Delta r_e &= r_e\left(\overline{R_{VIS}}, \overline{R_{SWIR}}\right) - \overline{r_e\left(R_{VIS,i}, R_{SWIR,i}\right)} \end{aligned}, \tag{3}$$

are considered in this, as well as previous studies, as the biases caused by the homogeneous pixel assumption in r_e and τ retrievals [8,10,12]

A UNIFIED MATHEMATICAL FRAMEWORK

The objective of this paper is to introduce a comprehensive framework that is able to reconcile and unify the theoretical understandings provided by Marshak et al. [8], Zhang and Platnick [9], and Zhang et al. [10] To investigate the sign and magnitude of $\Delta\tau$ and Δr_e, we first expand the $\tau\left(R_{VIS,i}, R_{SWIR,i}\right)$ and $r_e\left(R_{VIS,i}, R_{SWIR,i}\right)$ into two-dimensional Taylor series of $R_{VIS,i}$ and $R_{SWIR,i}$. Take $r_e\left(R_{VIS,i}, R_{SWIR,i}\right)$ for example. The expansion is:

$$
\begin{aligned}
r_e\left(R_{VIS,i}, R_{SWIR,i}\right) &= r_e\left(\overline{R_{VIS}} + \Delta R_{VIS,i}, \overline{R_{SWIR}} + \Delta R_{SWIR,i}\right) \\
&= r_e\left(\overline{R_{VIS}}, \overline{R_{SWIR}}\right) + \underbrace{\frac{\partial r_e\left(\overline{R_{VIS}}, \overline{R_{SWIR}}\right)}{\partial R_{VIS}} \Delta R_{VIS,i} + \frac{\partial r_e\left(\overline{R_{VIS}}, \overline{R_{SWIR}}\right)}{\partial R_{SWIR}} \Delta R_{SWIR,i}}_{\text{Linear terms}} + \\
&\quad \underbrace{\frac{1}{2}\frac{\partial^2 r_e\left(\overline{R_{VIS}}, \overline{R_{SWIR}}\right)}{\partial R_{VIS}^2} \Delta R_{VIS,i}^2 + \frac{\partial^2 r_e\left(\overline{R_{VIS}}, \overline{R_{SWIR}}\right)}{\partial R_{VIS}\,\partial R_{SWIR}} \Delta R_{VIS,i} \Delta R_{SWIR,i} + \frac{1}{2}\frac{\partial^2 r_e\left(\overline{R_{VIS}}, \overline{R_{SWIR}}\right)}{\partial R_{SWIR}^2} \Delta R_{SWIR,i}^2}_{\text{S econd-order terms}} + O\left(\Delta R^3\right)
\end{aligned}
\quad . \tag{4}
$$

If we take the spatial average of Eq. (4), all the linear terms (i.e., $\frac{\partial r_e\left(\overline{R_{VIS}}, \overline{R_{SWIR}}\right)}{\partial R_{VIS}} \Delta R_{VIS,i}$ and $\frac{\partial r_e\left(\overline{R_{VIS}}, \overline{R_{SWIR}}\right)}{\partial R_{SWIR}} \Delta R_{SWIR,i}$) vanish because $\overline{\Delta R_{VIS,i}} = \overline{\Delta R_{SWIR,i}} = 0$. Thus, only second order terms in Eq. (4) remain after the spatial average:

$$
\overline{r_e\left(R_{VIS,i}, R_{SWIR,i}\right)} \approx r_e\left(\overline{R_{VIS}}, \overline{R_{SWIR}}\right) + \frac{1}{2}\frac{\partial^2 r_e\left(\overline{R_{VIS}}, \overline{R_{SWIR}}\right)}{\partial R_{VIS}^2}\sigma_{VIS}^2 + \frac{\partial^2 r_e\left(\overline{R_{VIS}}, \overline{R_{SWIR}}\right)}{\partial R_{VIS}\,\partial R_{SWIR}}\operatorname{cov}\left(R_{VIS}, R_{SWIR}\right) + \frac{1}{2}\frac{\partial^2 r_e\left(\overline{R_{VIS}}, \overline{R_{SWIR}}\right)}{\partial R_{SWIR}^2}\sigma_{SWIR}^2 , \tag{5}
$$

where $\sigma_{VIS}^2 = \overline{\Delta R_{VIS,i}^2}$, $\sigma_{SWIR}^2 = \overline{\Delta R_{SWIR,i}^2}$ are the spatial variances of $R_{VIS,i}$ and $R_{SWIR,i}$, respectively, and $\operatorname{cov}\left(R_{VIS}, R_{SWIR}\right)$ is the spatial covariance of $R_{VIS,i}$ and $R_{SWIR,i}$. We obtain the following formula for Δr_e :

$$
\begin{aligned}
\Delta r_e &= r_e\left(\overline{R_{VIS}}, \overline{R_{SWIR}}\right) - \overline{r_e\left(R_{VIS,i}, R_{SWIR,i}\right)} \\
&= -\frac{1}{2}\frac{\partial^2 r_e\left(\overline{R_{VIS}}, \overline{R_{SWIR}}\right)}{\partial R_{VIS}^2}\sigma_{VIS}^2 - \frac{\partial^2 r_e\left(\overline{R_{VIS}}, \overline{R_{SWIR}}\right)}{\partial R_{VIS}\,\partial R_{SWIR}}\operatorname{cov}\left(R_{VIS}, R_{SWIR}\right) - \frac{1}{2}\frac{\partial^2 r_e\left(\overline{R_{VIS}}, \overline{R_{SWIR}}\right)}{\partial R_{SWIR}^2}\sigma_{SWIR}^2 \quad .
\end{aligned} \tag{6}
$$

Following the same procedure, we can derive the formula for $\Delta\tau$ as:

$$
\begin{aligned}
\Delta \tau &= \tau\left(\overline{R_{VIS}}, \overline{R_{SWIR}}\right) - \overline{\tau\left(R_{VIS,i}, R_{SWIR,i}\right)} \\
&= -\frac{1}{2}\frac{\partial^2 \tau\left(\overline{R_{VIS}}, \overline{R_{SWIR}}\right)}{\partial R_{VIS}^2}\sigma_{VIS}^2 - \frac{\partial^2 \tau\left(\overline{R_{VIS}}, \overline{R_{SWIR}}\right)}{\partial R_{VIS}\,\partial R_{SWIR}}\operatorname{cov}\left(R_{VIS}, R_{SWIR}\right) - \frac{1}{2}\frac{\partial^2 \tau\left(\overline{R_{VIS}}, \overline{R_{SWIR}}\right)}{\partial R_{SWIR}^2}\sigma_{SWIR}^2 \quad .
\end{aligned} \tag{7}
$$

Eq. (6) and (7) can be combined into a matrix form as follows:

$$
\begin{pmatrix} \Delta\tau \\ \Delta r_e \end{pmatrix} = \begin{pmatrix} -\frac{1}{2}\frac{\partial^2 \tau\left(\overline{R_{VIS}}, \overline{R_{SWIR}}\right)}{\partial R_{VIS}^2} & -\frac{\partial^2 \tau\left(\overline{R_{VIS}}, \overline{R_{SWIR}}\right)}{\partial R_{VIS}\,\partial R_{SWIR}} & -\frac{1}{2}\frac{\partial^2 \tau\left(\overline{R_{VIS}}, \overline{R_{SWIR}}\right)}{\partial R_{SWIR}^2} \\ -\frac{1}{2}\frac{\partial^2 r_e\left(\overline{R_{VIS}}, \overline{R_{SWIR}}\right)}{\partial R_{VIS}^2} & -\frac{\partial^2 r_e\left(\overline{R_{VIS}}, \overline{R_{SWIR}}\right)}{\partial R_{VIS}\,\partial R_{SWIR}} & -\frac{1}{2}\frac{\partial^2 r_e\left(\overline{R_{VIS}}, \overline{R_{SWIR}}\right)}{\partial R_{SWIR}^2} \end{pmatrix} \begin{pmatrix} \sigma_{VIS}^2 \\ \operatorname{cov} \\ \sigma_{SWIR}^2 \end{pmatrix} . \tag{8}
$$

Eq. (8) is the central equation of our framework for quantifying the impact of sub-pixel reflectance variance on r_e and τ retrievals. Eq. (8) decomposes the impact of sub-pixel cloud reflectance variability on the τ and r_e retrievals based on the bi-spectral method into two parts: 1) the magnitude of the sub-pixel reflectance variance and covariance specified by the vector $\left(\sigma_{VIS}^2,\ \operatorname{cov},\ \sigma_{SWIR}^2\right)^T$ (referred to as "sub-pixel variance vector") and 2) the matrix of the second-order derivatives of the LUT with respect to R_{VIS} and R_{SWIR} (referred to as "matrix of 2nd derivatives"). Given the LUT, the matrix of 2nd derivatives can be easily derived from straightforward numerical differentiation. An example of such a derived matrix based on the LUT for 0.86 µm reflectance ($R_{0.86}$) and 2.1 µm reflectance ($R_{2.1}$) is shown in The values of the 2nd derivatives for the grids of LUT are indicated by the color bar. Note that the sign of $\Delta\tau$ or Δr_e is determined both by the 2nd derivatives and the sub-pixel variance vector $\left(\sigma_{VIS}^2,\ \operatorname{cov},\ \sigma_{SWIR}^2\right)^T$. While σ_{VIS}^2 and σ_{SWIR}^2 are positive definite, the covariance term can be negative.

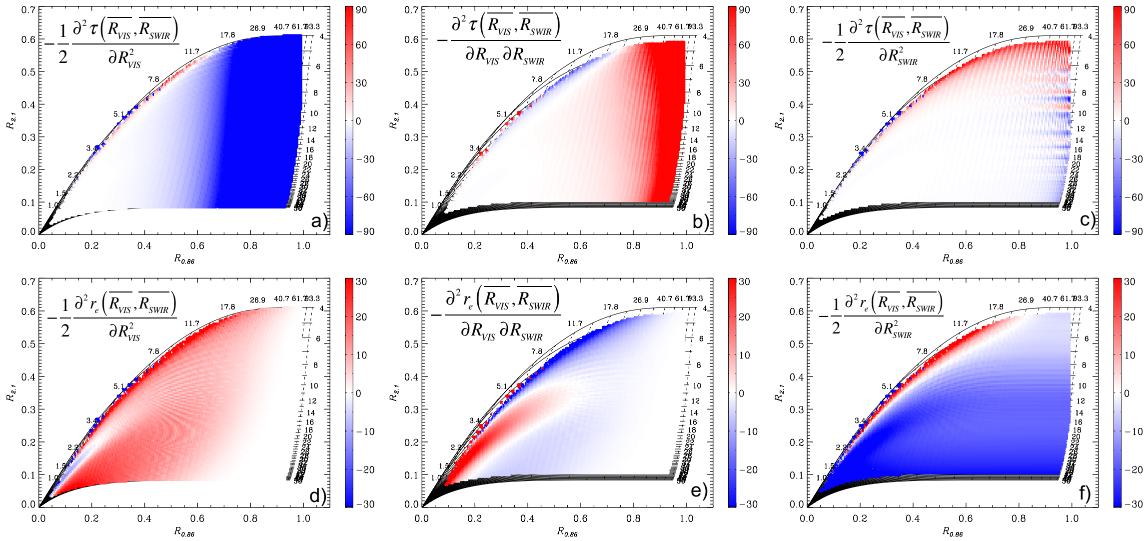

FIGURE 2. The sign and magnitude of each 2nd derivative term in Eq. *(8)* derived from the $R_{0.86}$ and R2.1 LUT. a) corresponds to $-\frac{1}{2}\frac{\partial^2\tau(\overline{R_{VIS}},\overline{R_{SWIR}})}{\partial R_{VIS}^2}$, *b) to* $-\frac{\partial^2\tau(\overline{R_{VIS}},\overline{R_{SWIR}})}{\partial R_{VIS}\,\partial R_{SWIR}}$, *c) to* $-\frac{1}{2}\frac{\partial^2\tau(\overline{R_{VIS}},\overline{R_{SWIR}})}{\partial R_{SWIR}^2}$, *d) to* $-\frac{1}{2}\frac{\partial^2 r_e(\overline{R_{VIS}},\overline{R_{SWIR}})}{\partial R_{VIS}^2}$, *e) to* $-\frac{\partial^2 r_e(\overline{R_{VIS}},\overline{R_{SWIR}})}{\partial R_{VIS}\,\partial R_{SWIR}}$, *and f) to* $-\frac{1}{2}\frac{\partial^2 r_e(\overline{R_{VIS}},\overline{R_{SWIR}})}{\partial R_{SWIR}^2}$. Solar and view zenith angles are assume to be 20° and 0°, relative azimuth angle is assumed to be 30° in these cases. (this figure is from Zhang et al. 2016[11])

It is clear from Eq. (8) that the τ and r_e retrievals are not only influenced by the sub-pixel variation of the primary band (i.e., R_{VIS} for τ and R_{SWIR} for r_e) but also by the variation of the secondary band (i.e., R_{SWIR} for τ and R_{VIS} for r_e), as well as the covariance of the two bands R_{VIS} and R_{SWIR}. Therefore, it reconciles and unifies the theoretical frameworks in Marshak et al. [8] and Zhang and Platnick [9] and Zhang et al. [10]. In particular, the impact of the PPHB on τ and r_e, described in Marshak et al. [8], corresponds to the upper-left term, $-\frac{1}{2}\frac{\partial^2\tau(\overline{R_{VIS}},\overline{R_{SWIR}})}{\partial R_{VIS}^2}$ **Fig. 2**a), and lower-right term, $-\frac{1}{2}\frac{\partial^2 r_e(\overline{R_{VIS}},\overline{R_{SWIR}})}{\partial R_{SWIR}^2}$ (**Fig. 2**f), in the 2nd derivatives matrix, respectively. As shown in **Fig. 2**, both terms are generally negative over the most part of LUT, consistent with the finding of Marshak et al. [8] that ignoring sub-pixel variability tends to result in an underestimation of the pixel average of the retrieved quantity if τ and r_e retrievals are considered separately and independently (i.e., negative $\Delta\tau$ and Δr_e). On the other hand, $\Delta\tau$ and Δr_e are also influenced by other terms in the matrix. For example, the $-\frac{1}{2}\frac{\partial^2 r_e(\overline{R_{VIS}},\overline{R_{SWIR}})}{\partial R_{VIS}^2}$ term in **Fig. 2**d is mostly positive in the region of the LUT with τ between about 1.5 and 20 and r_e between about 10 and 28 µm. This term competes with the negative $-\frac{1}{2}\frac{\partial^2 r_e(\overline{R_{VIS}},\overline{R_{SWIR}})}{\partial R_{SWIR}^2}$ term in determining the sign and size of Δr_e. In some cases, when σ^2_{VIS} is large as in the example in **Fig. 2**c, the influence of $-\frac{1}{2}\frac{\partial^2 r_e\left(\overline{R_{VIS}},\overline{R_{SWIR}}\right)}{\partial R^2_{VIS}}$ may be stronger, leading to a positive Δr_e, as argued in Zhang and Platnick [9] and Zhang et al. [10].

CONCLUSIONS AND SUMMARY

The impact of unresolved sub-pixel level variation of cloud reflectances is an important source of uncertainty in the bi-spectral solar reflective method. In this study, we develop a mathematical framework for understanding this impact and quantifying the consequent biases, $\Delta\tau$ and Δr_e. We show in Eq. (8) that $\Delta\tau$ and Δr_e are determined by two factors—the nonlinearity of the LUT and the inhomogeneity of reflectances within the pixel. We tested our framework using LES cloud fields and real MODIS observations. The results indicate that, in comparison with previous studies, our framework provides a more comprehensive explanation and also a more accurate estimation of the retrieval biases caused by the sub-pixel level variation of cloud reflectances[11]. Most importantly, it demonstrates that sub-pixel variations in cloud reflectance can lead to both positive and negative values of Δr_e. In both the LES and MODIS cases that we examined, Δr_e were dominantly positive, hence contributing to the dominantly positive bias in retrieved r_e from resolved cloud variability. Our framework could have several applications. For example, it can be used to understand the differences between retrievals made at different spatial resolutions (e.g., MODIS vs. SEVIRI) or based on different spectral reflectances (e.g., MODIS 2.1 µm vs. 3.7 µm). It could also useful for estimating retrieval uncertainties. For example, the retrieval uncertainty caused by sub-pixel reflectance variation in the operational 1 km MODIS cloud products can be estimated based on our framework from the 500 m cloud reflectances. It can also be integrated into the operational MODIS retrieval algorithm to determine in real-time whether the high-resolution retrievals (e.g., from 1km to 500m) are necessary for a given pixel. Such applications will be explored in future works.

ACKNOWLEDGEMENT

This research is supported by NASA grants NNX14AJ25G and NNX15AC77G

REFERENCES

1. T. Nakajima and M.D. King, J. Atmos. Sci. **47**, 1878 (1990).
2. Harshvardhan and D.A. Randall, Mon. Wea. Rev **113**, 1832 (1985).
3. R.F. Cahalan, W. Ridgway, W.J. Wiscombe, T.L. Bell, and J.B. Snider, J. Atmos. Sci. **51**, 2434 (1994).
4. H.W. Barker, Jas **53**, 2289 (1996).
5. L. Oreopoulos and R. Davies, Journal of Climate **11**, 919 (1998).
6. L. Oreopoulos, R.F. Cahalan, and S. Platnick, Journal of Climate **20**, 5114 (2007).
7. R. Pincus, S.A. McFarlane, and S.A. Klein, J. Geophys. Res. **104**, 6183 (1999).
8. A. Marshak, S. Platnick, T. Várnai, G. Wen, and R.F. Cahalan, J. Geophys. Res. **111**, D09207 (2006).
9. Z. Zhang and S. Platnick, J Geophys Res **116**, D20215 (2011).
10. Z. Zhang, A.S. Ackerman, G. Feingold, S. Platnick, R. Pincus, and H. Xue, J Geophys Res **117**, D19208 (2012).
11. Z. Zhang, F. Werner, H.M. Cho, G. Wind, S. Platnick, A.S. Ackerman, L. Di Girolamo, A. Marshak, and K. Meyer, Journal of Geophysical Research-Atmospheres 2016JD024837 (2016).
12. R.F. Cahalan and J.H. Joseph, Monthly Weather Review **117**, 261 (1989).